Current Scientific Research in Biomedical Sciences

Chembio Publishers
Right Choice for Researchers

Research Article *Volume 1; Issue 1*

Design of Porous Nano Cellulose Based Biopolymers for Nanomedicine Applications

Morais FP[1] and Curto JMR[1,2]*

[1]FibEnTech-Fiber Materials and Environmental Technologies Research Unit, University of Beira Interior, Portugal

[2]CIEPQPF- Chemical Process Engineering and Forest Products Research Centre, University of Coimbra, Portugal

***Corresponding author:** Professor Joana MR Curto, Department of Chemistry, Faculty of Science, University of Beira Interior, R. Marquês de Ávila e Bolama, 6201-001 Covilhã, Portugal, Tel no: +351 966 485 662; Email: joana.curto@ubi.pt

Received Date: October 18, 2018; **Published Date:** November 10, 2018

Abstract

The aim is to design nano fibrillated cellulose/carboxy methylcellulose (NFC/CMC) 3D porous biomaterials to be used in medicinal applications. NFC fibers were used to form a 3D nano matrix and CMC was used as an additive. The NFC/CMC concentration ratio proved to have influence on the 3D matrices hydrophilicity. Drug Delivery Systems (DDS) were formed using Diclofenac as the anti-inflammatory molecule. NFC/CMC 3D matrices were obtained with a combination of different fiber dimensions resulting in different structures with porosities ranging from 52 to 59%. The morphologic characterization of the fibers and the matrix structures was done using SEM and image analysis tools. The chemical characterization included the quantification of the total acidic groups using a conductivity method, FTIR-ATR spectroscopy and contact angle measurements. The representation of the 3D Diclofenac molecule was used to visualize the geometrical distribution of functional groups and the possibility of intermolecular interactions in the DDS formation, and also the influence of different pH surrounding environments.

A computational 3D simulation study of the porous NFC/CMC matrices was performed providing information about porosity and the pores dimensions. Using the computational information, the 3D porous systems were optimized to obtain the desired release kinetics, according to the different pH's, porosities and pore dimensions. Results proved that nanocellulosic porous materials can be designed according to the intended administration therapies and that the anti-inflammatory Diclofenac can be releases from the NFC/CMC 3D matrices with the desired kinetics, making the presented methodology applicable to different medicinal nano biomaterials.

Citation: Morais FP and Curto JMR. Design of Porous Nano Cellulose Based Biopolymers for Nanomedicine Applications. Curr Sci Res Biomed Sciences 2018, 1(1): 180003.

Graphical Abstract

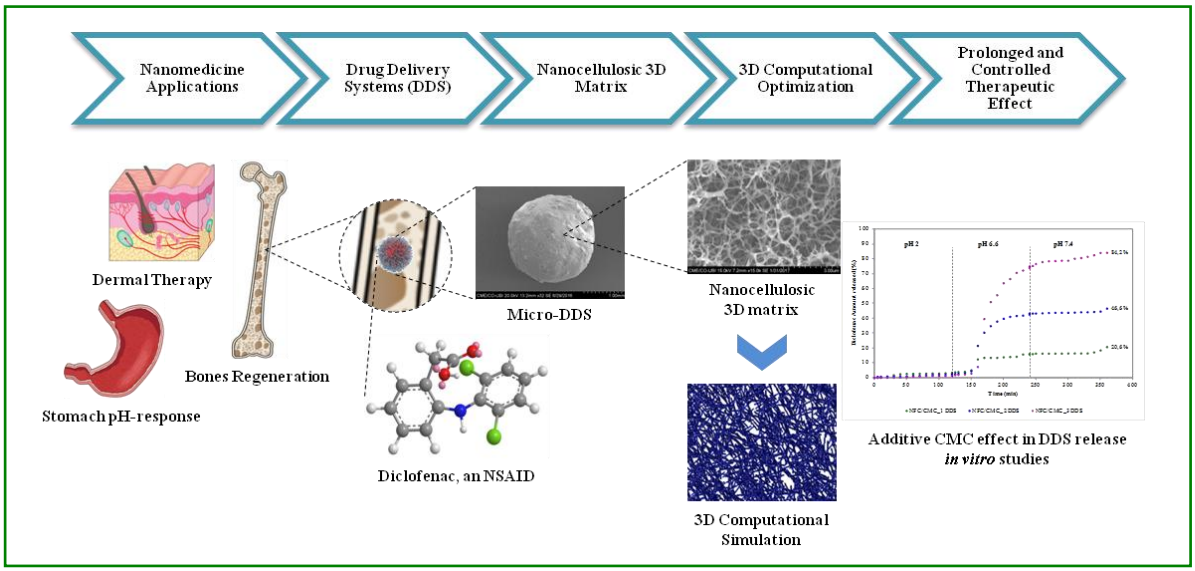

Keywords: Carboxy methylcellulose; Drug Delivery Systems; Nano fibrillated cellulose; Nano medicinal applications; Porosity

Abbreviations: CMC: Carboxy Methylcellulose; DDS: Drug Delivery Systems; NFC: Nano Fibrillated Cellulose; NSAID: Non-Steroidal Anti-Inflammatory Drug; SEM: Scanning Electron Microscopy; TEMPO: (2,2,6,6-Tetramethylpiperidin-1-yl)oxyl.

Introduction

The scientific interest in design and production of functional nanosystems with the goal of effectively retaining, transporting, delivering and directing therapeutic molecules has been growing in recent years with applications in biomedical, nanomedicine and pharmaceutical systems [1,2]. The use of biopolymers in nanomedicine is a growing research field, because these materials have substantially different properties compared to other conventional materials, including passive accumulation at local target and personalized engineering solutions for specific clinical requirements [3-5]. The extensive versatility of biopolymers expands new innovative horizons to infections, tissue regeneration, bone reconstruction, cell growth,and skin treatments, for example[6-10]. The nanomedicine applications contribute to more effective diagnoses, as well as to the reduction of therapeutic doses, using drug delivery systems (DDS), and reducing the associated adverse side effects.The design of biopolymers porous materials for biomedical applications, such as DDS and scaffolds, present the challenge to obtain the porous materials with control pore dimensions and distribution [11-14]. The high surface area and the porosity allow enhancing cell adhesion [15]. The creation of 3D matrices with all the morphological and physiological factors allows a faster cellular growth and development, with the most suitable medium for each tissue [16].

The nanofibers matrices production is very important in tissue engineering [17]. In bone regeneration, the matrices must have properties such as mechanical strength, pore dimension and tree-dimensional (3D) architecture [11,18,19]. The articular cartilage has little capacity for regeneration due to low vascularization and cells capable of producing new cartilage. Therefore, the incorporation of specific cells into 3D matrices is a good alternative to produce new cartilage [20,21]. Also the use of 3D matrices whose nanofibers are aligned promotes the regeneration of connective tissues responsible for joint movement and stability [22]. A promising example capable of producing a 3D matrix is nanocellulose.

Nano fibrillated cellulose (NFC) is a biopolymer that can be manipulated benefiting the nanotechnology development and be used in innovative materials development [23]. Nanocellulose has several characteristics including porosity, high specific surface area, specific orientation, surface chemical reactivity,

biocompatibility, biodegradability, absence of toxicity, among others [24]. Nanocellulose can also be widely applied in medical implants like stent, tissue engineering, DDS, wound healing, cardiovascular applications, as well as other medical applications [25-31]. For example, bones are 3D composed materials with three distinct kinds of cells: osteoclasts, osteoblasts and osteocytes. When a bone fractures the construction of the bone is done by the osteoclasts and, like every cell, it takes time to multiply. The use of 3D structures, like nanocellulose DDS, that can mimic the properties of the bone and improve regeneration, can be a turn event in the regeneration medicine [9]. Furthermore, cosmetics and skin treatments are others applications where nanocellulose can be employed [32], since nanocellulose is already successfully applied as a healing for wet sores as burns, allowing deep penetration of the skin by different active substances [33].

The nanocellulose chemical modification can achieve derivatives with different properties and applications. Carboxymethylcellulose (CMC) is an example of such derivatives, which is obtained by replacing the hydroxyl groups with carboxymethyl groups [34]. This biopolymer has high chemical stability, safety, absence of toxicity, biocompatibility, biodegradability and solubility, and can be applied in, pharmaceutical and biomedical fields [34,35]. The use of CMC as an additive to form a NFC/CMC 3D matrix is a promising research due to its potential in different applications. The encapsulation and formation of a nanocellulosic biomaterials combined 3D matrix in a DDS, capable of releasing controlled therapeutics, is a promising investigation for the DDS targeting to the different desired applications.

Nano biomaterials have great importance in the field of nanomedicine due to their small dimension, high surface area and charge, among other properties, which make them efficient DDS [15]. In this context, the goal of present study was to characterize and investigate NFC's suitability as a 3D matrix nanocellulosic biomaterial, using CMC as an additive in different concentrations, in DDS for different applications in nanomedicine, such as bone regeneration, dermal therapy and targeting in the stomach. Diclofenac, 2-[2-(2,6-dichloroanilino)phenyl]acetic acid, was the therapeutic molecule selected because it is a highly prescribed non-steroidal anti-inflammatory drug (NSAID) and because it has associated gastric adverse side effects. Alginate was used as a cross linking biopolymeric agent, creating a stabilized structure, capable of incorporating the nanocellulose 3D matrix with the optimized porosity and pore dimensions, and releasing the drug with the desired controlled kinetics.

The conjugation of the biopolymers contributed to the formation of a DDS with a tailored made 3D matrix and diffusion barrier, decreasing the migration of the therapeutic molecules [36]. The morphological, biometric and chemical characterization and kinetic studies were performed, demonstrating the potential of NFC/CMC 3D matrix in different applications. Molecular modeling and computational simulations were used to predict and develop the 3D nanocellulose matrices [37]. The structure porosity and pore dimensions were studied using SEM information and a 3D fibrous materials computational simulator [37,38]. The use of computational tools helped to reducethe number of laboratory experiments and to obtain optimized structures and tailored made release kinetics.

Materials and Methods

Materials

Kraft Eucalyptus globulus pulp, was obtained by FibEnTech Research Unit, University of Beira Interior, Covilhã, Portugal. CMC sodium salt, high viscosity (1500-3000) cP in 1% H_2O (25^oC) and Diclofenac sodium salt (>99%) were purchased from Sigma Aldrich (Germany). Alginate sodium salt, with high viscosity,was acquired by BDH Chemicals Ltd (England). All other chemicals and reagents used in the study were analytical grade.

Production of NFC gel and NFC/CMC gel

NFC suspension was obtained by deconstructing the vegetable cellulose (*Kraft Eucalyptus globulus* pulp) by beating according to ISO 5264/2 standard, followed by a chemical treatment using (2,2,6,6-Tetramethylpiperidin-1-yl)oxyl (TEMPO)-mediated oxidation [39]. Cellulose fibers suspension was exposed to TEMPO and sodium bromide (NaBr). A certain amount of 9% sodium hypochlorite solution (NaClO) was added slowly. Solution pH was monitored and maintained at 10.5 at controlled temperature (addition of small amounts of sodium hydroxide (NaOH)). Thereafter, a 0.5M hydrochloric acid (HCl) solution was added to adjust the pH to 7. Subsequently, a high pressure homogenizer (GEA, 50L7h @ 1500 bar) was used in the mechanical treatment. This step was carried out with recirculation, 500 bar pressure and a constant cooling water flow.

The operating temperature was between 20 and 40 °C and it was controlled to avoid products degradation. The NFC suspension was densified using a Buchner funnel with pre-weighed filter paper with control of stirring, temperature, time and pressure, producing a gel-like NFC structure.

CMC solutions with different concentrations (CMC_1: 0.1% (w/v), CMC_2: 0.01% (w/v), CMC_3: 0.001% (w/v)) were prepared. An amount of CMC_1 was added to the NFC suspension,stirring overnight. NFC/CMC_1 gel is obtained under the same conditions described above. The same procedure was performed for NFC/CMC_2 and NFC/CMC_3 gel.

Production of DDS

DDS were produced using an alginate solution, to obtain the crosslinked polymer, the NFC/CMC_1in form of a gel, containing the 3D nanocellulose matrix, and the therapeutic molecule (the Diclofenac), in a 2:1:2 ratios. The mixture was added dropwise to a 0.2M calcium chloride ($CaCl_2$) solution and the resulting microspheres were left in this solution for 24 h [40]. Finally, the DDS were filtered, rinsed with distilled water anddried. The same procedure was performed for NFC/CMC_2 and NFC/CMC_3DDS.

Biometric and morphological characterization

Scanning electron microscopy (SEM): To maintain the porous structure, samples were immersed in a glutaraldehyde solution overnight. Subsequently, ethanol solutions of graduated concentrations were used to replace the water with ethanol in the samples. The samples were dried by CO_2 Critical Point Drying method, using EMS K850 Critical Point Drier equipped with thermo-electronic heating, adiabatic cooling and temperature control of +5^{o}C in cooling and +35^{o}C during heating [41]. After this treatment, the samples were placed on an aluminum support using a double-sided adhesive tape. The samples were coated with gold using a Sputter Quorum Q 15 OR ES (Quorum Technologies, United Kingdom) to become conductors and were analyzed using a SEM S-2700 Hitachi (Tokyo, Japan), operating at 20 kV and at different magnifications.

Image analysis: SEM images were processed and analyzed using image analysis software for fibers and pores characterization. “Esprit” from “Bruker” was used to determine pore dimensions, “DiameterJ” and “ImageJ” were usedfor fibers and pore dimensions. SEM images were processed using a methodology withdefined criteria for the stabilization of the average of the measured values.

Chemical characterization

Total Acid Groups quantification: A conductivity titration method was carried out according to SCAN-CM 65 (Scan-test, 2002) standard, adjusted to thequantity of materials involved. NFC gel was suspended in HCl solution for 15 minutes. The suspension was then filtered and washed with deionized water.The filtrate was recycled to remove excess acid. The process was carried out until the conductivity was less than 5μS/cm. Distilled water and a certain amount of sodium chloride (NaCl) solution were added to the sample. The suspension was titrated with a solution of NaOH, with drops of 0.1 mL, added for 10 to 30 seconds, and the conductivity was recorded after each addition. Titration terminated when the suspension reached a pH value of 10.5. The procedure was done in duplicate.

Fourier-transform infrared spectroscopy with attenuated total reflectance (FTIR-ATR): FTIR-ATR was performed, using Thermo-Nicolet IS10 equipment, with 32 scans, with a resolution of 4 cm^{-1} and a wavelength range of 600 to 4000 cm^{-1}.

Contact angle: The contact angle method was performed to evaluate the water interaction and contact angle of different structures, using aOCAH200, Data physics equipment. The method was performed with0.52 cm distance, 0.5μL/s feed and 5μL drop volume.

Computational studies

Molecular modeling: The ChemDraw Ultra 1.2 software was used to represent the Diclofenac. Minimum energy conformations structures, formation energy, molecular electrostatic potentials, partial atomic charges and electrostatic potentials 3D maps were analyzed.

3D computational simulation: A 3D simulator of fibrous materials [37] was used to study the influence of porosity and pore distribution on nanocellulose DDS 3D matrices. The 3D simulator uses as input parameters the fibers dimensions and produces the resulting 3D structure made from these fibers. A computational experimental design was implemented to study the effect of the NFC 3D matricesin the DDS. The simulation studies provided information about porosity and pore dimensions in 3D matrix for one thousand simulated structures. The results were organized in regression trees and several 3D matrices were selected to be produced in the laboratory, having the desired porosity and more regular pore distribution, resulting in more effective DDS.

Kinetic studies

Drug release *in vitro* studies

Kinetic studies were performed in triplicate for 6h with controlled temperature ((37±0.5) ^{o}C) and homogenization (100 rpm). Buffer solutions with pH valuesof 2 (stomach), 6.6 (duodenum) and 7.4 (blood stream) were used to test the different body fluids [42]. Throughout the assay, various aliquots were removed, the volume was restored with the same amount of liquid that was removed,and analyzed by UV-Vis spectroscopy method (276 nm) using

a Helios Omega UV-Vis spectrophotometer and a quartz cell with an optical path of 1 cm.

Swelling studies: The DDS were weighed at the beginning (W_1) and at the end (W_2) of the kinetics studies, carefully removing excess water on its surface using a tissue paper. The swelling index (%) was calculated using Eq. (1) [43].

Swelling index (%) = $((W_2 - W_1) / W_1) * 100$ (1)

Results and Discussion

Biometric and morphological characterization

The experimental gel structures were obtained from two different biopolymers, NFC and CMC, with different fibrillation degree. Figure 1 shows an example of the gel structure obtained with NFC and CMC solution. NFC gel consists of long, flexible and entangled cellulose nanofibrillated fibers. This gel is a biomaterial with a random and porous 3D matrix where the binding effect between the fibers is visible in SEM. This NFC gel structure depended on the pre-treatment applied for its production. The applied methods promoted and increased the accessibility of hydroxyl groups, the internal surface and the reactivity of fibers, as verified in previous studies [44].

CMC is going to be used in this work as an additive, in small percentages, to study the ability to change the affinity with water. CMC is crystalline cellulose that in solution forms a viscous gel with an interlaced, uniform and open 3D matrix, showing visible differences with the NFC gel, capable of transporting molecules inside of the gel. Kono (2014) also reported that CMC hydrogels showed water retention capacity inside of the gel when the structure had a regular and uniform porosity [45]. The goal was to produce a 3D NFC/CMC matrix structure with the best combination of the structural properties like porosity, pore dimensions, distribution and uniformity. The nanofibrillated matrices, using CMC as an additive showed the potential of production structures capable of capturing large quantities of therapeutic molecules because of their high porosity and OH bonding.

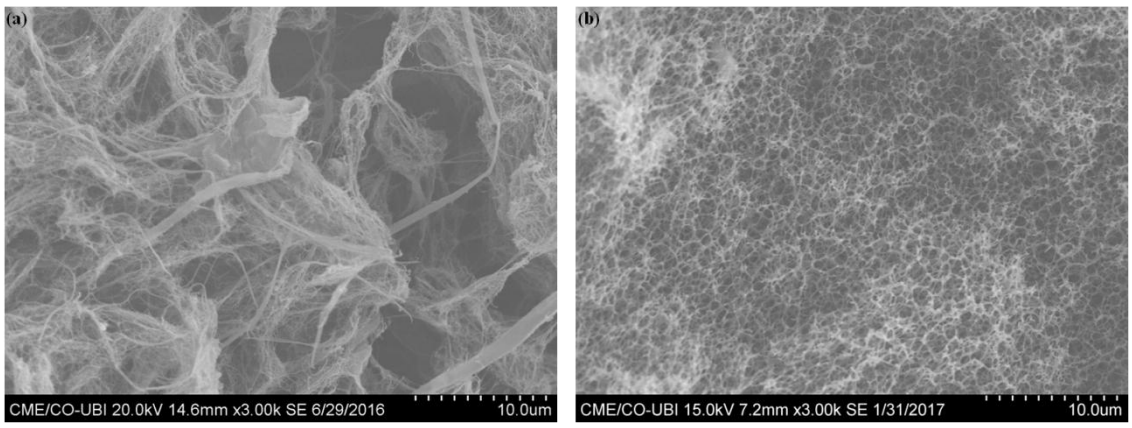

Figure 1: SEM images of NFC gel 3D matrix (a) and CMC 3D matrix (b) (magnification: 3000x).

DDS containing 3D nanocellulosic matrices and Diclofenac were evaluated for particle size and surface morphology. The addition of metal ions method produced DDS with diameter ranging from 1 to 2 mm. Figure 2a showed an example of DDS, exhibiting a spherical cross linking structure. Through transversal sections of DDS was possible to observe the incorporated 3D nanocellulosic matrix (Figure 2b-d). The addition of CMC at different concentrations modified the 3D nanocellulosic matrices. The NFC/CMC_1 gel 3D matrix formed a regular, random and porous layer structure with similarities to the NFC gel 3D matrix. The NFC/CMC_2 gel 3D matrix and the NFC/CMC_3 gel 3D matrix showed similarities to the CMC 3D matrix since they formed an entangled, uniform and open 3D matrix. Increasing the amount of added CMC to the NFC matrix became the NFC/CMC matrices more closely knit, with differences in fiber diameters. Chen et al. reported similar events in CMC interference in bacterial cellulose structures. They concluded that CMC significantly modified the structure of this cellulose, becoming the 3D matrix denser, which facilitated water absorption [46].

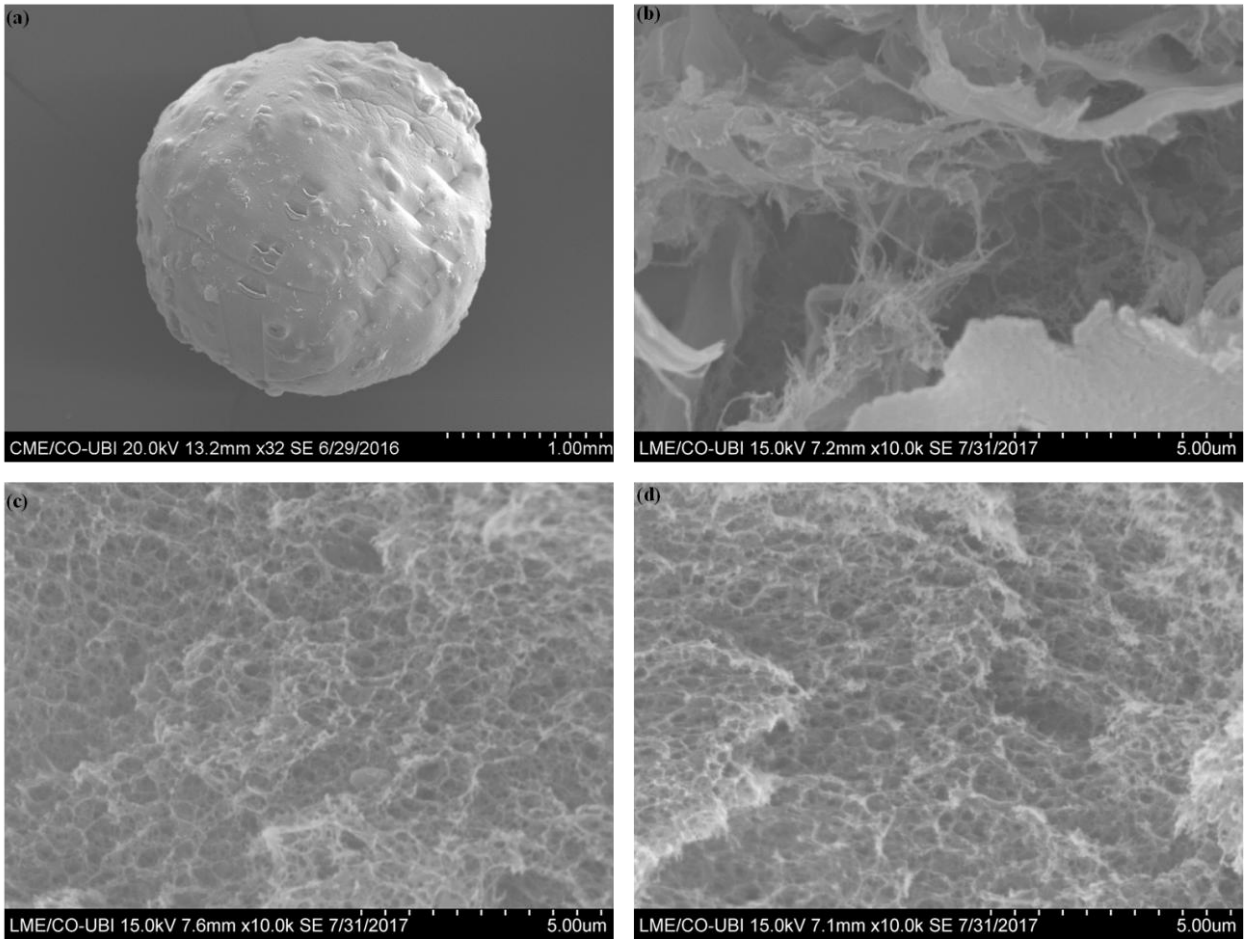

Figure 2: SEM images of DDS (a), NFC/CMC_1 gel 3D matrix (b), NFC/CMC_2 gel 3D matrix (c) and NFC/CMC_3 gel 3D matrix (d) (magnifications: 32x and 10000x).

The SEM binary experimental structures of 3D NFC/CMC matrices were quantified and analyzed using image analysis tools (Table 1), resulting in different structures with porosities varying from 52 to 59%. The fibers and pores of each 3D NFC/CMC matrices were selected to be statistically representative, obtaining differences in width, length and area. The results indicated that pore dimensions and distribution depend on the fibers dimensions. The NFC/CMC_1 3D matrix fibers showed superior widths and lengths, followed by NFC/CMC_3 3D matrix and NFC/CMC_2 3D matrix. Both fibers widths and lengths presented different distributions, in nanoscale order (less than 100 nm). The NFC/CMC_3 3D matrix pores presented superior average area, followed by NFC/CMC_2 3D matrix and NFC/CMC_1 3D matrix. Consequently, a larger average surface area corresponds to a larger porosity.

The results also indicated that porosity can be changed with the addition of different concentrations of CMC. Different porosities also correspond to different release kinetics, for example, Diclofenac faster release kinetics corresponds to the NFC/CMC_3 DDS, matrix with a higher porosity. This quantification process was essential to 3D nanocellulosic matrix optimization in DDS through computational simulation studies. The fiber dimensions data were used as input parameters in the computational simulator and the output parameters, like porosity, were used to computational validation and obtain the desired 3D nanocellulosic matrices for the different nanomedicine applications. The possibility of biomaterials optimized design can be done using this methodology, combined experimental and computational characterization techniques, as it will be reported shortly.

			NFC/CMC$_1$	NFC/CMC$_2$	NFC/CMC$_3$
Fibers	Width (nm)	Min	9.9	9.9	9.9
		Max	504.5	542.4	613.3
		Average	93.4±0.046	70.7±0.033	71.9±0.036
	Length (nm)	Min	5.0	5.0	4.9
		Max	1189.0	1024.0	945.8
		Average	211.0±0.174	157.0±0.125	162.4±0.126
Pores	Area (nm^2)	Min	0.3	0.3	8.7
		Max	784.2	537.7	2913.7
		Average	32.9±0.093	52.1±0.309	276.9±0.633
	Porosity (%)		52.46	54.19	59.13

Table 1: Fiber and pore properties of NFC/CMC$_1$, NFC/CMC$_2$ and NFC/CMC$_3$ 3D matrices.

Chemical characterization

The NFC gel was obtained by a combination of mechanical micro fibrillation and chemical TEMPO-mediated oxidation pre-treatment. The carboxylic groups (COOH) content determination presented a value of 328 µmol/g, TEMPO oxidation facilitated defibrillation, increasing the carboxylic groups content on the NFC surface, being in agreement with several studies reported in the literature [44].

The FTIR-ATR technique was used to analyze the differences in the functional groups of biomaterials used in the study. Figure 3 shows the FTIR spectra of NFC and CMC. NFC FTIR spectra showed a band at 3324.82 cm^{-1} corresponding to the OH groups' bonds vibration [47] and at 2893.50 cm^{-1} corresponding to the C-H groups' bonds vibration. The band found at 1645.85 cm^{-1} corresponds to the carboxylic acid groups (C=O and C-O) bonds stretching.

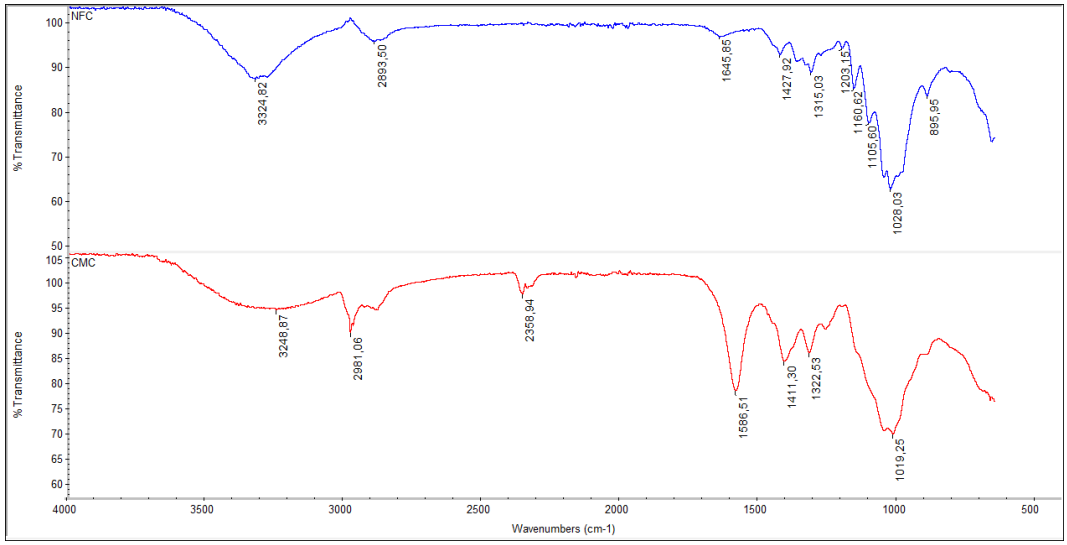

Figure 3: NFC and CMC FTIR-ATR spectrum.

The presence of this band is due to TEMPO-mediated oxidative treatment as part of the NFC production process [44]. The asymmetric absorption bands at 1427.92 and 1315.03 cm^{-1} correspond to the carboxylic acid salt groups, namely COONa, found after the chemical treatment. The bands at 1028.03 cm^{-1} and 895.95 cm^{-1} are also associated with the vibrations of the C-O and C-H cellulose polymer bonds present in the polymer chain. CMC FTIR spectra showed at 3248.87 cm^{-1} an OH group stretch vibration band, while the band assigned to the C-H stretch occurred in the region between 2981.06 cm^{-1}. The intense bands at 1411.30 cm^{-1} and 1322.53 cm^{-1} refer to the CH_2 and OH groups folding vibration, respectively. At around 1019.25 cm^{-1} the band observed is probably due to the CH-O-CH_2 stretch. The spectrum also showed a band at 1586.51 cm^{-1} which is attributed to the COO- group antisymmetric vibration.

The biomaterials chemical modification can be used to change the 3D structure as well as increase the affinity with water. The addition of cellulose derivatives, such as CMC, leads to the modification of the available surface groups, which influence solubility, facilitating biomaterials hydration. Previous studies have verified that the CMC addition in celluloses of microbial origin presents changes in the affinity with water [46,48]. To the best of our knowledge the addition of CMC to NFC has been poorly investigated. In this work, the surface hydrophobicity was evaluated by the surface contact angle measurement. If the contact angle is less than 70°, the biomaterials surface is considered hydrophilic, if the opposite is true, the surface is considered hydrophobic [49].

This property is important for the therapeutic molecules selection to be incorporated into DDS and intermolecular interactions with the surrounding environment. The contact angle for each structure is shown in Table 2. NFC presented as the least hydrophilic structure, indicative of a more closed 3D matrix structure, with OH groups available on the surface. When CMC was added to the NFC structure, the structure became more hydrophilic, indicative of the presence of more OH groups available for interaction with water. The contact angle results indicate that CMC is an additive with the ability to increase water affinity and intermolecular interactions. Fornanocellulose structures, with different fibrillation degrees, the interaction with water depends on several factors, which will contribute in different ways to the total amount of OH groups available on the surface.

Biomaterials	Contact Angle (º)
NFC	65.28±3.36
NFC/CMC	47.31±3.26

Table 2: NFC and CMC contact angle values.

Computational studies

Molecular modeling is an important tool for understanding therapeutic molecules chemical theories [50,51]. By understanding the Diclofenac chemistry it is possible to optimize the DDS structural properties in order to achieve the desired therapeutic effect. Diclofenac has a bridged secondary amino group with two aromatic rings, representing the intra molecular hydrogen bonds source towards one chlorine atom and one carboxyl group of the other aromatic ring [52]. Through the Diclofenac molecular study it was possible find the most stable Diclofenac 3D conformation in the state of minimum potential energy, with a formation value of -31.8213 kcal/mol (Figure 4).

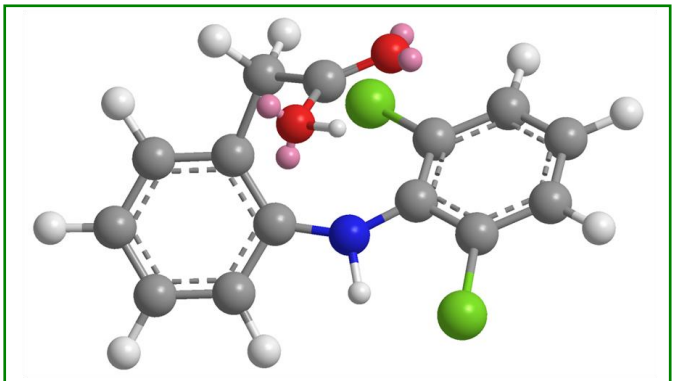

Figure 4: Diclofenac 3D chemical structure in the lower energy state.

Partial atomic charges distribution to Diclofenac molecule was also determined (Table 3). From this analysis the amino group (N8) and oxygen atoms (O18 and O19) were identified as being a preferred nucleophilic local for interactions.

Atoms	Charges	Atoms	Charges
C1	-0.140	C11	0.308
C2	-0.056	C12	0.019
C3	0.071	C13	0.127
C4	0.055	C14	-0.138
C5	-0.157	C15	0.112
C6	0.019	C16	-0.048
Cl7	0.064	C17	-0.042
N8	-0.309	O18	-0.164
Cl9	0.020	O19	-0.156
C10	0.026		

Table 3: Diclofenac partial atomic charges population analysis.

Positive charge point interaction with Diclofenac nucleotides and electrons were determined by molecular electrostatic potentials based on the charge density calculated directly from the molecular wave function [53]. Diclofenac higher nucleophilicity region (Figure 5, in red) is an electron-rich region. Therefore, this local is more conducive for molecular interactions.

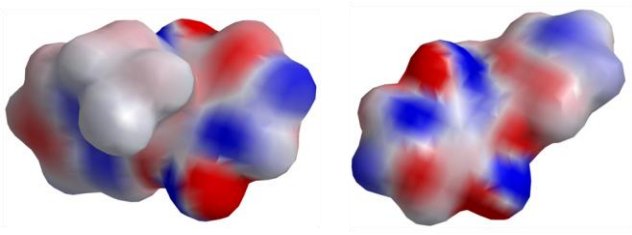

Figure 5: Diclofenac electrostatic potential map.

The highest orbitals participating in the molecules chemical stability are the highest occupied molecular orbital (HOMO) and the lowest unoccupied molecularorbital (LUMO). HOMO is capable of donating an electron while LUMO accepts electrons. HOMO and HOMO -1 exhibit a π-bond molecular orbital and LUMO and LUMO +1 exhibit a π* molecular orbital. The Diclofenac HOMO -1, HOMO, LUMO and LUMO +1 orbital energies are -10,546, -7,644, +0,100, +0,783 eV, respectively. The orbital energy gap LUMO and HOMO has a value -7,544 eV. Figure 6 represents these molecular orbitals for Diclofenac, showing positive phases in red and negative phases in blue.

A computational simulation study was performed to optimize the DDS 3D matrix. The integration of SEM image analysis data was essential to form 3D structures in the computational simulator [37]. The 3D structure was formed by the deposition of nanofibers. Depending on its position, dimension and flexibility, the fiber adjusted to the underlying structure, occupying the free space above the already deposited fibers, as it happens in the NFC gel production process. The fibers are positioned randomly to simulate the formation of 3D structures produced in the laboratory. The porosity was well visible in the NFC/CMC 3D simulated matrices. The porosity is calculated using the ratio of voids, or voxels without fibers, and the total amount of voxels.

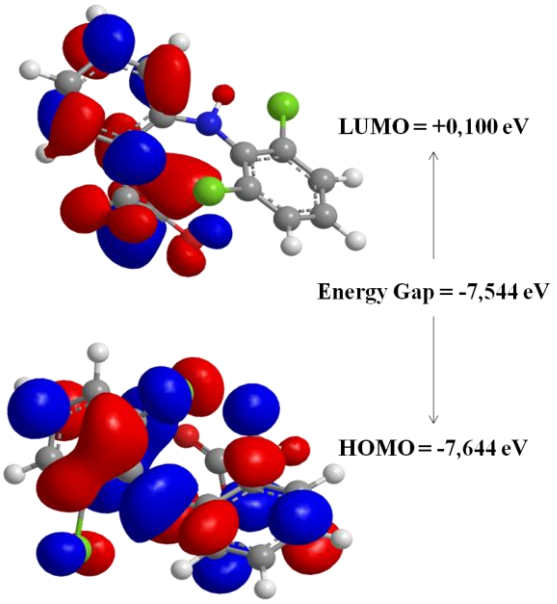

Figure 6: Diclofenac HOMO and LUMO.

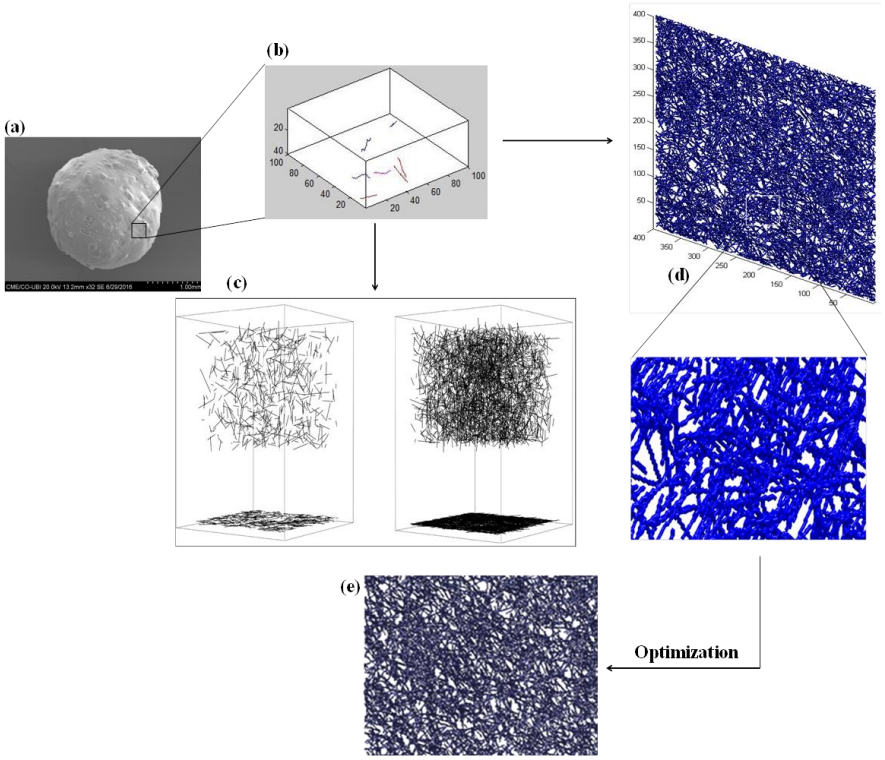

Figure 7: Scheme of the computational simulator.(a)DDS 3D biopolymer matrix obtained experimentally (b) the deposition of fibers in matrix (c) 3D simulations of the fiber structures (adapted from [54]) (d) computational porous matrix (e) detail of the 3D matrix.

To study the influence of several input parameters in the formation of the 3D matrices, the computational simulator was used to obtain the structures computationally (Figure 7). Using the 3D matrices porosity analysis as the desired output, the simulator was used to modify the input variables, and several scenarios were simulated and analyzed. The structures were than produced in the laboratory, saving time and resources. The results were organized using regression trees to understand how it would be possible with the same fibrous elements to obtain several possibilities for the porosity. Pore dimensions and its distribution proved to be very important parameters for the design of structures with regular release kinetics. Structures with higher pore dimension variability release the therapeutic molecules in different rates, because they will have different path lengths associated with different pore dimensions of the nanocellulose 3D matrix. The biopolymeric 3D matrix computational simulation studies indicated that a matrix with a more regular pore distribution could be obtained with the same fibrous elements. These structures were produced in the laboratory, controlling the conditions of the 3D matrix formation, by manipulation of the filtration process variables. These matrices, obtained with more regular pore dimension, resulted in more uniform controlled release kinetics.

The results indicate that the porosity and pore dimension are important for the DDS performance. Therefore, the computational simulator was used to produce structures with the desired pore dimension and these results were used to develop and produce the 3D matrices in the laboratory. This methodology can be used to design porous materials for other nano medicinal applications.

Kinetic studies

The *in vitro* Diclofenac release studies of NFC/CMC_1 DDS, NFC/CMC_2 DDS and NFC/CMC_3 DDS showed 21%, 47% and 84%, respectively, drug release within 6h, in the different dissolution media. The release profiles were similar at pH 2, indicating the absence of release at this pH, but exhibited different drug release kinetics and drug retentions, for pH 6.6 and 7.4 (Figure 8).

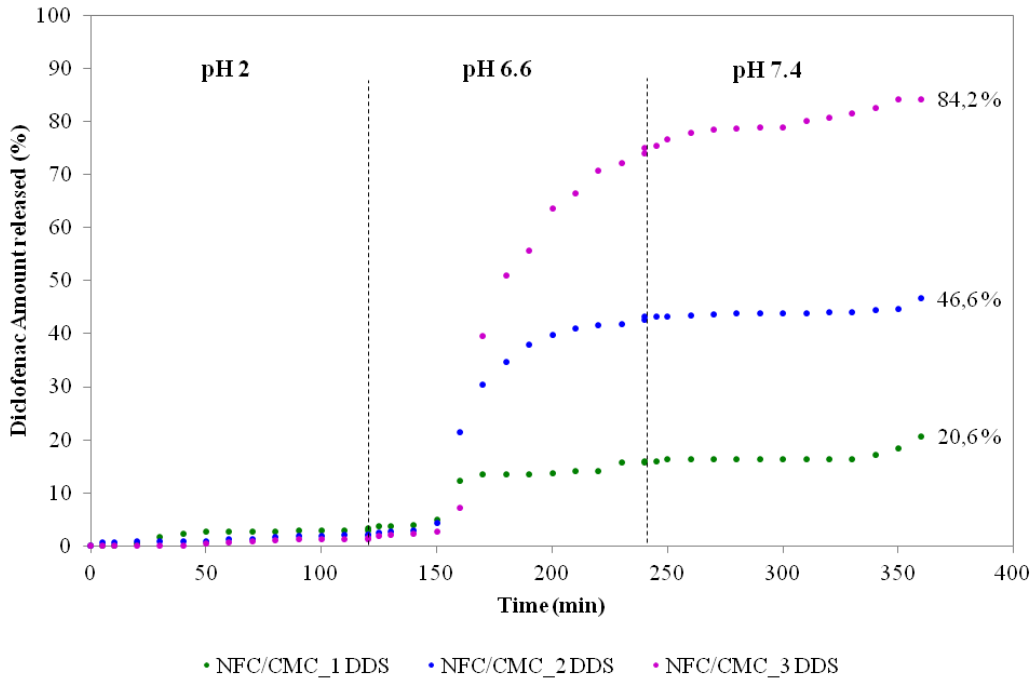

Figure 8: Diclofenac release *in vitro* studies from NFC/CMC_1 DDS, NFC/CMC_2 DDS and NFC/CMC_3 DDS at different pH mediums.

For different applications in nanomedicine, the methodology to produce the DDS presented in this work can be efficient to obtain the drug transport and release in the body, according to the patient needs. The purpose was to incorporate Diclofenac into the nanocellulose 3D matrix, to control the Diclofenac release it at the desired pH and to reduce the associated adverse effects with the release at the acidic stomach pH. Diclofenac when administered orally has a high incidence of adverse side effects on the gastrointestinal tract because it is not stable

in the stomach acidic environment. The production of a delivery system that decreases its release into the gastrointestinal tract (pH 2) is an advantage when oral drug targeting exists. At pH 2, when the system is used as a DDS in oral administrations, it showed near zero release, which indicates that the system presented advantages for its application as DDS in oral therapeutics. At pH 6.6, the anti-inflammatory molecule Diclofenac is releases in a controlled way, presenting meaningful differences for each system, which means that the system can be tailored made for different therapeutic applications, when the target is the duodenum absorption. At pH 7.4, which mimics the bloodstream pH, the results indicate a regular and controlled release over time, which is an advantage when the molecule is administered topically, implanted in the bones or in the circulatory system. The results indicate that the nanofibrillated cellulose DDS is able to release the anti-inflammatory molecule in a regular way, prolonging its therapeutic effect and avoiding the release at the stomach acid pH. The side effects associated with anti-inflammatory drugs, like Diclofenac, can be partially overcome with the use of a system that targets and controls its release.

The swelling studies of NFC/CMC1 DDS, NFC/CMC2 DDS and NFC/CMC3 DDS were carried out throughout the dissolution assay (Figure 9). In swelling mechanism the drug release rate depends on the amount of surrounding medium entering the biopolymer matrix [55]. The NFC/CMC1 DDS, NFC/CMC2 DDS and NFC/CMC3 DDS of approximately 69%, 58% and 54% swelling index, respectively. These values indicated that the affinity with water can be controlled using CMC as an additive. The swelling and Diclofenac release had a directly and inversely proportional behavior, respectively, relative to the amounts of CMC present, behavior that is in accordance to the described in the literature [56].

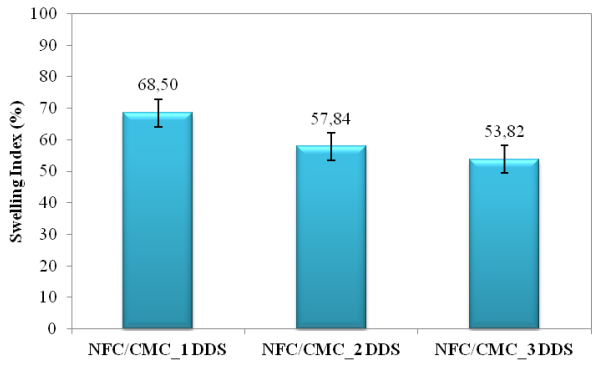

Figure 9: Swelling index for NFC/CMC_1 DDS, NFC/CMC_2 DDS and NFC/CMC_3 DDS.

Conclusion

The produced NFC/CMC 3D matrices were designed to incorporate and transport he therapeutic molecule Diclofenac. The addition of CMC to the NFC matrices modified its hydrophilicity, resulting in DDS with increased water affinity. The incorporation of NFC/CMC 3D matrices in the alginate-based DDS structure allowed the development of systems capable of releasing the therapeutic molecule in a controlled way, with an more steady anti-inflammatory activity. The DDS produced were activated by the pH surrounding environment. At low pH the DDS had a near-zero release of Diclofenac, which is beneficial for oral therapy, avoiding the undesired stomach side effects of non steroid anti-inflammatory therapies. Therefore, the DDS can be targeted to have a therapeutical effect and release according to the surrounding environment ph. These controlled release of anti-inflammatory drugs, with uniform release over a period of time, may be useful in other porous systems, like for example in bone regeneration therapies, porous flexible systems like “stents” or dermal therapeutic applications, allowing drug administration to be done in a safe and uniform way.

The simulator was able to model the structural elements of 3D NFC/CMC matrices and proved to be an efficient way to predict the porosity of the structures. The simulation results were organized using decision/regression trees and from these, several structures were selected because of their porosity, pore dimension and pore distribution. These structures were made on the laboratory and presented different kinetics, making it possible to establish` a relation between the 3D matrix structure and the release kinetics, with considerable time and resources economy.

References

1. Doshi N, Mitragotri S (2009) Designer Biomaterials for Nanomedicine. Advanced Functional Materials 19(24): 3843-3854.

2. Lima AC, Alvarez-Lorenzo C, Mano JF (2016) Design Advances in Particulate Systems for Biomedical Applications. Adv Healthc Mater 5(14): 1687-1723.

3. De Jong WH, Borm PJ (2008) Drug delivery and nanoparticles: applications and hazards. Int J Nanomedicine 3(2): 133-149.

4. Owen A, Rannard S, Bawa R, Feng SS (2015) Interdisciplinary nanomedicine publications through interdisciplinary peer-review. Journal of Inter disciplinary Nanomedicine 1(1): 4-8.

5. Larrañeta E, McCrudden MT, Courtenay AJ, Donnelly RF (2016) Microneedles: A New Frontier in NanomedicineDelivery. Pharm Res 33(5): 1055-1073.

6. Markman JL, Rekechenetskiy A, Holler E, Ljubimova JY (2013) Nanomedicine therapeutic approaches to overcome cancer drug resistance. Adv Drug Deliv Rev 65(13-14): 1866-1879.

7. Liu J, Huang Y, Kumar A, Tan A, Jin S, et al. (2014) pH-Sensitive nano-systems for drug delivery in cancer therapy. Biotechnol Adv 32(4): 693-710.

8. Azzopardi EA, Conlan RS, Whitaker IS (2016) Polymer therapeutics in surgery: the next frontier. J Interdiscip Nanomed 1(1): 19-29.

9. Lavrador P, Gaspar VM, Mano JF (2018) Stimuli-responsive nanocarriers for delivery of bone therapeutics - Barriers and progresses. J Control Release 273: 51-67.

10. Ribeiro C, Borges J, Costa AMS, Gaspar VM, Bermudez VZ, et al. (2018) Preparation of Well-Dispersed Chitosan/Alginate Hollow Multilayered Microcapsules for Enhanced Cellular Internalization. Molecules 23(3): E625.

11. Hollister SJ (2005) Porous scaffold design for tissue engineering. Nat Mater 4(7): 518-524.

12. Dvir T, Timko BP, Kohane DS, Langer R (2011) Nanotechnological strategies for engineering complex tissues. Nat Nanotechnol 6(1): 13-22.

13. Han N, Johnson J, Lannutti JJ, Winter JO (2012) Hydrogel-electrospun fiber composite materials for hydrophilic protein release. J Control Release 158(1): 165-170.

14. Kreuter J (2014) Drug delivery to the central nervous system by polymeric nanoparticles: what do we know? Adv Drug Deliv Rev 71: 2-14.

15. Vasita R, Katti DS (2006) Nanofibers and their applications in tissue engineering. Int J Nanomedicine 1(1): 15-30.

16. Rexeisen EL, Fan W, Pangburn TO, Taribaqil RR, Bates FS, et al. (2010) Self-assembly of fibronectin mimetic peptide-amphiphile nanofibers. Langmuir 26(3): 1953-1959.

17. Moroni L, Schotel R, Hamann D, Wijn JR, van Blitterswijk CA (2008) 3D Fiber-Deposited ElectrospunIntegrated Scaffolds Enhance Cartilage Tissue Formation. Advanced Functional Materials 18(1): 53-60.

18. Cheng Q, Benson DR, Rivera M, Kuczera K (2006) Influence of point mutations on the flexibility of cytochrome b5: molecular dynamics simulations of holoproteins. Biopolymers 83(3): 297-312.

19. Casper CL, Yang W, Farach-Carson MC, Rabolt JF (2007) Coating electrospun collagen and gelatin fibers with perlecan domain I for increased growth factor binding. Biomacromolecules 8(4): 1116-1123.

20. Barnes CP, Sell SA, Boland ED, Simpson DG, Bowlin GL (2007) Nanofiber technology: designing the next generation of tissue engineering scaffolds. Adv Drug Delive Rev 59(14): 1413-1433.

21. Kunzmann A, Andersson B, Thurnherr T, Krug H, Scheynius A, etal. (2011) Toxicology of engineered nanomaterials: focus on biocompatibility, biodistribution and biodegradation. Biochim Biophys Acta 1810(3): 361-373.

22. Ayres CE, Jha BS, Sell SA, Bowlin GL, Simpson DG (2010) Nanotechnology in the design of soft tissue scaffolds: innovations in structure and function. Wiley Interdiscip Rev Nanomed Nanobiotechnol 2(1): 20-34.

23. Lin N, Dufresne A (2014) Nanocellulose in biomedicine: Current status and Future prospect. European Polymer Journal 59: 302-325.

24. Dufresne A (2013) Nanocellulose: A new ageless bionanomaterial. Materialstoday 16(6): 220-227.

25. Österberg M, Cranston ED (2014) Special Issue on Nanocellulose- Editorial. Nord Pulp Pap Res J 29(1): 1-2.

26. Jorfi M, Foster EJ (2015) Recent advances in nanocellulose for biomedical applications. Journal of Applied Polymer Science 132(14): 41719.

27. Kim JH, Shim BS, Kim HS, Lee YJ, Min SK, et al. (2015) Review of nanocellulose for sustainable future materials. International Journal of Precision Engineering and Manufacturing-Green Technology 2(2): 197-213.

28. Abitbol T, Rivkin A, Cao Y, Nevo Y, Abraham E, et al. (2016) Nanocellulose, a tiny fiber with huge applications. Curr Opin Biotechnol 39: 76-88.

29. Debele TA, Mekuria SL, Tsai HC (2016) Polysaccharide based nano gels in the drug delivery system: Application as the carrier of pharmaceutical agents. Mater Sci Eng C Mater Biol Appl 68: 964-981.

30. Mondal S (2017) Preparation, properties and applications of nanocellulosic materials. Carbohydr Polym 163: 301-316.

31. Hu T, Yang C, Lin S, Yu Q, Wang G (2018) Biodegradable stents for coronary artery disease treatment: Recent advances and future perspectives. Mater Sci Eng C Mater Biol Appl 91: 163-178.

32. Ioelovich M (2016) Nanocellulose – fabrication, structure, properties, and application in the area of care and cure. In: Grumezescu AM (Ed.), Fabrication and Self-Assembly of Nanobiomaterials: Applications of Nanobiomaterials. (1st Edn), William Andrew Publishing, New York, USA, pp. 243-288.

33. Ludwicka K, Jedrzejczak-Krzepkowska M, Kubiak K, Kolodziejczyk M, Pankiewicz T, et al. (2016) Medical and Cosmetic Applications of Bacterial NanoCellulose. In: Bielecki S, et al. (Eds.), Bacterial Nanocellulose: From Biotechnology to Bio-Economy, Elsevier, pp. 145-165.

34. Halib N, Perrone F, Cemazar M, Dapas B, Farra R, et al. (2017) Potential Applications of Nanocellulose-Containing Materials in the Biomedical Field. Materials (Basel) 10(8): 977.

35. Butun S, Ince FG, Erdugan H, Sahiner N (2011) One-step fabrication of biocompatible carboxymethyl cellulose polymeric particles for drug delivery systems. Carbohydrate Polymers 86(2): 636-643.

36. Tonnesen HH, Karlsen J (2002) Alginate in drug delivery systems. Drug Dev Ind Pharm 28(6): 621-630.

37. Curto JMR, Conceicao ELT, Portugal ATG, Simoes RMS (2011) Three dimensional modelling of fibrous materials and experimental validation. Materialwissenschaft und Werkstofftechnik 42(5): 370-374.

38. Curto JMR, Mendes AO, Conceição ELT, Portugal ATG, Fiadeiro PT, et al. (2015) Development of an Innovative 3D Simulator for Structured Polymeric Fibrous Materials and Liquid Droplets. In: Ochsner A & Altenbach H (Eds.), Mechanical and Materials Engineering of Modern Structure and Component Design - Advanced Structured Materials, Springer International Publishing, Germany, pp. 301-321.

39. Pierre G, Punta C, Delattre C, Melone L, Dubessay P, et al. (2017) TEMPO-mediated oxidation of polysaccharides: An Ongoing Story. Carbohydr Polym 165: 71-85.

40. Vijayalakshmi K, Gomathi T, Sudha PN (2014) Preparation and characterization of nanochitosan/sodium alginate/microcrystalline cellulose beads. Der Pharm Lett 6(4): 65-77.

41. Gomide Junior MH, Sterzo EV, Macari M, Boleli IC (2004) Use of Scanning Electron Microscopy for the Evaluation of Intestinal Epithelium Integrity. Revista Brasileira de Zootecnia 33(6): 1500-1505.

42. González-Rodríguez ML, Holgado MA, Sánchez-Lafuente C, Rabasco AM, Fini A (2002) Alginate/chitosan particulate systems for sodium diclofenac release. Int J Pharm 232(1-2): 225-234.

43. Mehta R, Chawla A, Sharma P, Pawar P (2013) Formulation and in vitro evaluation of Eudragit S-100 coated naproxen matrix tablets for colon-targeted drug delivery system. J Adv Pharm Technol Res 4(1): 31-41.

44. Abdul Khalil HPS, Davoudpour Y, Islam N, Mustapha A, Sudesh K, et.al. (2014) Production and modification of nanofibrillated cellulose using various mechanical processes: A Review. Carbohydrate Polymer 99: 649-665.

45. Kono H (2014) Characterization and properties of carboxymethyl cellulose hydrogels crosslinked by polyethylene glycol. Carbohydr Polym 106(1): 84-93.

46. Chen HH, Chen LC, Huang HC, Lin SB (2011) In situ modification of bacterial cellulose nanostructure by adding CMC during the growth of *Gluconacetobacter xylinus*. Cellulose 18(6): 1573-1583.

47. Ciolacu D, Ciolacu F, Popa VI (2011) Amorphous Cellulose – Structure and Characterization. Cellulose Chemistry and Technology 45(1-2): 13-21.

48. Cheng KC, Catchmark JM, Demirci A (2011) Effects of CMC addition on bacterial cellulose production in a biofilm reactor and its paper sheets analysis. Biomacromolecules 12(3): 730-736.

49. Hansen D, Bomholt N, Jeppesen JC, Simonsen AC (2017) Contact angle goniometry on single micron-scale fibers for composites. Applied Surface Science 392: 181-188.

50. Leach AR (2001) Molecular Modeling: Principles and Applications (2nd Edn), Harlow, England.

51. Ooms F (2000) Molecular modeling and computer aided drug design. Examples of their applications in medicinal chemistry. Curr Med Chem 7(2): 141-158.

52. Fini A, Cavallari C, Ospitali F (2010) Diclofenac Salts. V. Examples of Polymorphism among Diclofenac Salts with Alkyl-hydroxy Amines Studied by DSC and HSM. Pharmaceutics 2(2): 136-158.

53. Politzer P, Truhlar DG (1981) Chemical Applications of Atomic and Molecular Electrostatic Potentials: Reactivity, Structure, Scattering, and Energetics of Organic, Inorganic, and Biological Systems (1st Edn), Springer, New York, United States.

54. Sampson WW (2001) The structural characterisation of fibre networks in papermaking processes - A review. 12th Fundamental Research Symposium – Paper as a Network, Oxford, pp. 1205-1288.

55. Coelho JF, Ferreira PC, Alves P, Cordeiro R, Fonseca AC, et al. (2010) Drug delivery systems: Advanced technologies potentially applicable in personalized treatments. EPMA J 1(1): 164-209.

56. Efentakis M, Vlachou M, Choulis NH (1997) Effects of Excipients on Swelling and Drug Release from Compressed Matrices. Drug Development and Industrial Pharmacy 23(1): 107-112.